Published in final edited form as:
J Neurobiol. 2006 December ; 66(14): 1630–1645. doi:10.1002/neu.20309.

Developmental Regulation of Sensory Axon Regeneration in the Absence of Growth Cones

Steven L. Jones[1], **Michael E. Selzer**[2], and **Gianluca Gallo**[1]

1*Department of Neurobiology and Anatomy, Drexel University College of Medicine, Philadelphia, Pennsylvania 19129*

2*Department of Neurology, University of Pennsylvania, Philadelphia, Pennsylvania 19104*

Abstract

The actin filament (F-actin) cytoskeleton is thought to be required for normal axon extension during embryonic development. Whether this is true of axon regeneration in the mature nervous system is not known, but a progressive simplification of growth cones during development has been described and where specifically investigated, mature spinal cord axons appear to regenerate without growth cones. We have studied the cytoskeletal mechanisms of axon regeneration in developmentally early and late chicken sensory neurons, at embryonic day (E) 7 and 14 respectively. Depletion of F-actin blocked the regeneration of E7 but not E14 sensory axons *in vitro*. The differential sensitivity of axon regeneration to the loss of F-actin and growth cones correlated with endogenous levels of F-actin and growth cone morphology. The growth cones of E7 axons contained more F-actin and were more elaborate than those of E14 axons. The ability of E14 axons to regenerate in the absence of F-actin and growth cones was dependent on microtubule tip polymerization. Importantly, while the regeneration of E7 axons was strictly dependent on F-actin, regeneration of E14 axons was more dependent on microtubule tip polymerization. Furthermore, E14 axons exhibited altered microtubule polymerization relative to E7, as determined by imaging of microtubule tip polymerization in living neurons. These data indicate that the mechanism of axon regeneration undergoes a developmental switch between E7 and E14 from strict dependence on F-actin to a greater dependence on microtubule polymerization. Collectively, these experiments indicate that microtubule polymerization may be a therapeutic target for promoting regeneration of mature neurons.

Keywords

actin; growth cone; regeneration; microtubule; EB3; transport; dynamic instability

INTRODUCTION

Growth cones are motile structures required for embryonic axon extension and guidance (Gallo and Letourneau, 2004). Axon extension requires assembly and reorganization of the cytoskeleton (Dent and Gertler, 2003). In developing axons, actin filaments (F-actin) are concentrated at the growth cone. The axon contains microtubules, neurofilaments, and sparse F-actin. Polymerization of F-actin and microtubules occurs largely in the distal axon, the growth cone. Whether growth cones are required for axon regeneration in the mature nervous system is not known. However, a progressive simplification of growth cones during

Correspondence to: G. Gallo..

This article contains supplementary material available via the Internet at http://www.interscience.wiley.com/jpages/0022-3034/suppmat.

development has been described (Mason, 1985; Nordlander, 1987; Gorgels, 1991), and where looked for, axons appear to regenerate without growth cones. Specifically, regenerating axons in the lamprey spinal cord extend without growth cones or F-actin, but the tips contain microtubules and neurofilaments (Lurie et al., 1994; Hall et al., 1997; Zhang et al., 2005). Thus, the role of F-actin in axon regeneration is not clear and might vary with the developmental age of neurons.

Marsh and Letourneau (1984) and Letourneau et al. (1987) demonstrated that embryonic day 9–11 chicken sensory neurons can regenerate axons *in vitro* under conditions of depleted F-actin, albeit at much slower rates. Similar results have been obtained in a variety of other neuronal systems (Abosch and Lagenaur, 1993; Bradke and Dotti, 1999; Ruthel and Hollenbeck, 2000; Zmuda and Rivas, 2000). The cytoskeletal organization of regenerating lamprey axons *in vivo* is similar to that observed when F-actin is depolymerized *in vitro* (Marsh and Letourneau, 1984; Lurie et al., 1994; Hall et al., 1997; Zhang et al., 2005). Collectively these observations indicate that some regenerating axons may extend by an F-actin-independent mechanism and emphasize the importance of understanding the mechanism of axon extension in the absence of F-actin (Selzer, 2003).

Components of the neuronal cytoskeleton undergo developmentally regulated expression (e.g., microtubule associated proteins; Emery et al., 2003). However, the functional significance of changes in cytoskeletal components or dynamics has not been clarified. When axons reach their target tissues, extension stops and axon arbor elaboration commences. This switch is likely mediated by changes in the regulation of the neuronal cytoskeleton. Indeed, during embryogenesis dorsal root ganglion neurons transition from extending a few long projecting axons to multiple highly branched axons (Bray et al., 1987; Smith and Skene, 1997). Furthermore, the ability of postnatal axons to extend in vitro is diminished relative to embryonic axons (Argiro and Johnson, 1982; Argiro et al., 1984; Kleitman and Johnson, 1989), suggesting changes in the mechanism of axon extension.

We investigated the cytoskeletal basis of axon regeneration at two developmental stages of dorsal root ganglion neurons in vitro. The data demonstrate that early (embryonic day 7: E7) axons strictly require F-actin for axon maintenance and regeneration. However, E14 axons continue to extend in the absence of F-actin. Investigations of developmental changes in microtubule dynamics, and functional experiments, indicate that the ability of E14 axons to extend under conditions of depleted F-actin is due to developmentally regulated changes in the dynamics of the microtubule cytoskeleton. These observations have implications for our understanding of the mechanistic basis of axon regeneration in the mature nervous system and suggest the hypothesis that developmentally older axons may regenerate through a mechanism less dependent on F-actin than younger axons.

METHODS

Culturing and Reagents

Explants and dissociated cells of chicken embryonic dorsal root ganglia were prepared and cultured as previously detailed (Lelkes et al., 2006). Briefly, substrata were coated with 25 μg/mL laminin in phosphate-buffered saline or 100 μg/mL polylysine (Sigma, St. Louis) overnight at 39°C. All experiments were performed in defined F12 Ham medium with supplements. For live imaging experiments, cultures were prepared using “video dishes” (Falcon 1006 plates with glass coverslip bottoms).

Latrunculin A (LatA; Molecular Probes, Eugene OR), swinholide A (Molecular Probes), vinblastine (VB; Sigma), and cytochalasin D (CD; Sigma) were stored as stocks at -20°C at concentrations 1000-fold greater than that used in experiments.

Phase Contrast Videomicroscopy

For live imaging of axon extension, cultures were placed on an inverted Zeiss 135M microscope (Zeiss, Gottingen Germany; 20× phase objective) in series with an Axiocam CCD camera (Zeiss) and a PC unit operating AxionVision software (Zeiss). The stage was heated at 39°C using an ASI-400 air curtain (NevTek Burnsville, VA). Axon extension rates were determined using the measurement module of AxioVision by determining the total length of axon formed between fixed time points (imaging interval 1 min). Extension rates were analyzed using the Welch *T*-test that does not assume equal variances.

Fluorescence Microscopy

Neurons transfected with fluorescent constructs were studied by time-lapse fluorescence imaging using a Zeiss 200M microscope with a Zeiss three-plate insert heated-stage, and objective heater, and equipped with an Orca ER CCD camera (Hamamatsu, Bridgewater NJ). All fluorescence-imaging data acquisition and analysis were performed using Zeiss AxioVision software. Acquisition and analysis of fluorescently labeled cultures were similarly performed on a Zeiss 200M microscope. A 100× oil objective was used for image acquisition.

Cytochemistry

In order to specifically detect polymeric tubulin, cultures were simultaneously fixed and extracted, as described in Gallo and Letourneau (1999), in cytoskeletal stabilizing buffer. Blocking was performed for 1 h and antibodies were applied for 1 h in the protocols described below, all at room temperature. To detect F-actin and microtubules, cultures were stained with rhodamine—phalloidin (1 h, 8 μL/100 μL; Molecular Probes) and DMA1-A anti tubulin (1:100 FITC-conjugated primary; Sigma). In experiments using dissociated cells, neuronal tubulin was stained using a monoclonal antibody specific to neuronal βIII tubulin (1:400 TUJ; Sigma) and secondary FITC-conjugated goat—anti-mouse antibody (1:400; Sigma). For double labeling of neurofilament M (NF-M) and tubulin, cultures were fixed with 4% paraformaldehyde containing 5% sucrose. NF-M was detected by indirect fluorescence using the monoclonal 446 antibody (1:400; ATCC Hybridoma Bank, Manassas, VA) and secondary rhodamine-conjugated goat—anti-mouse antibody (1:400; Sigma). For double labeling with anti-neurofilament, tubulin staining was performed using a sheep—anti-tubulin polyclonal antibody (1:200; Sigma) and secondary FITC-conjugated rabbit—anti-sheep antibody (1:200; Sigma). Samples were blocked in 10% goat serum, or 10% rabbit serum (for neurofilament staining), containing 0.1% Triton X-100 in phosphate-buffered saline.

For double labeling of tyrosinated or acetylated tubulin relative to total tubulin, we used monoclonal anti-tyrosine tubulin (1:400 TUB-1A2; Sigma) and anti-acetylated tubulin (1:100 6-11B-1; Sigma), respectively. Total tubulin was labeled using a polyclonal rabbit—anti-tubulin antibody (1:40; Sigma). For these staining experiments, cultures were simultaneously fixed and extracted, blocked with goat serum, and then stained with antibodies to posttranslational modification of tubulin and total tubulin. Secondary antibodies were then applied (1:400 rhodamine-conjugated goat—anti-mouse and 1:200 FITC-conjugated sheep—anti-rabbit; Sigma). All stained preparations were mounted in NoFade medium and stored at -20°C.

Quantification of Fluorescent Staining

Quantification of growth cone F-actin content was performed as described in Ernst et al. (2000). Similarly, microtubule content was determined as in Gallo and Letourneau (1999). All quantitative measurements were obtained using the measurement module of AxioVision Software (Zeiss). Briefly, regions of interest were determined and the mean pixel intensity of staining determined, following subtraction of background signal. The mean intensity was then

multiplied by the area in pixels to determine the integrated total intensity within the region of interest. Unless otherwise noted, data were analyzed using the Welch *T*-test that does not assume equal variances.

Transfection

EB3-GFP plasmids were a kind gift of Dr. P.W. Baas (Drexel University; Stepanova et al., 2003). Plasmids were prepared using standard methods (Qiaprep kit, Qiagen, Valencia CA). EB3-GFP plasmids were electroporated into neurons, using the Amaxa Nucleofector (setting G13; Amaxa, Gaithersburg, MD). Dissociated cells from 40 dorsal root ganglia were transferred to an Amaxa transfection cuvette in transfection medium supplemented with 10 μg of plasmid DNA, electroporated, and immediately transferred to culturing medium. The dissociated cells were then routinely plated in six video dishes and cultured overnight.

Imaging and Quantification of EB3 Comet Dynamics

Live imaging of EB3-GFP was performed on an Axiovert 200M (Zeiss) microscope using a 100× objective with minimal light from a 100 W bulb and EGFP-filter sets (Chroma Technology, Rockingham, VT). Quantification of EB3 comet advancement rates and lifespans was performed in the distal region of axons (~100 μm) excluding the growth cones. We chose axons instead of growth cones as our sampling domain because microtubule—F-actin interactions in growth cones may affect the behavior of microtubule tips in unpredicted ways (Hasaka et al., 2004), while the axons provide a relatively homogeneous domain with sparse actin filaments. Furthermore, axons provide a relatively linear environment for microtubule tip polymerization unlike growth cones that constantly change shape and provide a barrier to microtubule advance beyond the leading edge. EB3 comet lifespans were analyzed essentially as previously described (Stepanova et al., 2003; Hasaka et al., 2004). EB3 comet lifespans were determined by measuring the total time between comet formation and comet disappearance. Comet formation comprised a change in fluorescence intensity from a homogenous low level to a bright comet-like appearance and occurred on the scale or 1–2 s. The lifespan of EB3 comets was considered terminated when the comet was no longer detectable above the axonal background. Comets that seemed to immediately reappear after having been undetected during the previous two intervals (6 s) were considered new comets. EB3 comet advancement rates were determined using Axiovision software by determining the total distance of advancement during comet lifespans. Measurements were obtained by totaling the distance of advancement that occurred during each interval and then dividing the total distance by the total time (lifespan).

RESULTS

E7 DRG Growth Cones are More Complex and Contain More F-Actin than E14 Growth Cones but Extend at Similar Rates

Previous reports identified a correlation between decreases in growth cone complexity and decreased axon regeneration rates *in vitro* between embryonic and postnatal neurons (Argiro and Johnson, 1982; Argiro et al., 1984). In our study, we investigated growth cone morphology, F-actin content, and axon extension rates in early (E7) and late (E14) embryonic chicken DRG raised in nerve growth factor. We chose E7 as our earliest time point because neuronal proliferation in chicken DRG terminates at E7, and E7 thus represents a time point when neurons have proliferated but have not undergone significant differentiation and are actively extending toward their target tissue (Carr and Simpson, 1978), although some axons have reached the still developing target tissue. On the other hand, by E14 axons have reached their peripheral target and arborized. Furthermore, dissociated cultured chicken DRG undergo a transition from projecting a single axon to multiple axons between E7 and E14 (not shown; consistent with Bray et al., 1987). The transition from extension of a single to multiple axons

is characteristic of later stages of DRG neuron differentiation (Smith and Skene, 1997; Bomze et al., 2001). Axon extension on laminin, but not polylysine, is dependent on integrin receptors (Kuhn et al., 1998). We therefore compared the effects of age on both substrata to rule out developmental changes in integrin expression or function (Guan et al., 2003). *In vitro* sensory axons are effectively regenerating as they have undergone severing during the dissection required to extract the ganglia from the embryos.

A comparison of the morphology of growth cones from E7 and E14 DRG revealed an age-related decrease in growth cone complexity [Fig. 1(A,B)]. The changes in morphology were independent of substratum (laminin *vs*. polylysine). Axon extension/regeneration on laminin is dependent on integrin signaling while on polylysine axons attach to the substratum through nonspecific electrostatic interactions (Kuhn et al., 1998). Thus developmental changes observed *in vitro* on both laminin and polylysine are not likely to reflect changes in integrin-mediated signaling. On laminin, E7 growth cones exhibited 107% greater number of filopodia than does E14 growth cones, and the area of E7 growth cones was 86% greater than that of E14 growth cones [Fig. 1(A,B)]. On polylysine, E7 growth cones exhibited 228% more filopodia than does E14 growth cones, and the size of E7 growth cones was 146% greater that of E14 growth cones [Fig. 1(A,B)].

Growth cone morphology is dependent on F-actin. However, changes in growth cone morphology or size are not necessarily related to changes in the amount of F-actin present in growth cones. Quantification of total F-actin content revealed that E7 growth cones contain 86% and 263% more F-actin than E14 growth cones on laminin and polylysine, respectively [Fig. 1(C)].

To determine whether the striking differences in growth cone morphology and F-actin content between E7 and E14 growth cones are related to the mechanism of axon regeneration, we measured the rates of extension of E7 and E14 axons on laminin and polylysine. Axons from both E7 and E14 DRG extended at similar rates on both laminin and polylysine [Fig. 1(D)]. The rate at any given age was determined by the substratum with axons extending faster on laminin than polylysine [Fig. 1(D)]. These data demonstrate that growth cone complexity and F-actin content are not major regulators of axon extension rate during the developmental period under study.

F-Actin Depletion Severely Disrupts E7 but not E14 Axon Maintenance and Extension

E7 growth cones are more complex and contain more F-actin than E14 has, although the rates of axon extension do not differ between the two developmental ages. However, the relative differences in F-actin content between E7 and E14 axons may reflect a role for F-actin independent of the regulation of axon extension. Therefore, we determined the effects of depletion of F-actin on E7 and E14 axons using CD and LatA on axon extension. CD causes F-actin depolymerization by capping the barbed ends of actin filaments and LatA binds soluble actin rendering it polymerization incompetent (Coue et al., 1987; Spector et al., 1989). Depletion of F-actin was confirmed by phalloidin staining. LatA uniformly decreased staining intensity by 95% throughout the axon (not shown). CD treatment also significantly decreased F-actin levels, although small residual F-actin clumps were observed (not shown). DRG explants were treated with CD or LatA for 24 h starting at 24 h after plating when axons were ~1-mm long. Chronic F-actin depolymerization resulted in marked retraction of E7 axons on both laminin and polylysine [Fig. 2(A)]. E7 axons that remained under these conditions were thin and invariably failed to extend [Fig. 2(B)]. In contrast, although E14 axons underwent some retraction in response to chronic F-actin depolymerization, axons were able to extend even following 24-h treatment with LatA or CD [Fig. 2(B)]. These data demonstrate that E7 but not E14 axons require F-actin for maintenance and extension independent of substratum.

We next tested whether F-actin depletion would differentially alter the ability of dissociated neurons to regenerate axons as a function of developmental age. E7 and E14 neurons were dissociated and plated on polylysine and laminin coated substrata in the presence of DMSO (control) or CD. Following overnight culturing, the cultures were fixed and stained with neuron-specific tubulin (βIII) antibodies. The percentage of neurons extending axons was then determined. CD treatment decreased axon formation by 80% and 15% in E7 and E14 cultures, respectively [Fig. 2(C); x^2, $p < 0.001$]. Collectively, these data demonstrate that actin filament depletion affects both the initial regeneration and later maintenance of axons and the effects are significantly greater in E7 than E14 axons.

Effects of F-Actin Depolymerization on Neurofilament and Microtubule Organization in E7 and E14 Axons

In order to gain insight into the differences in the effects of F-actin depletion on E7 and E14 axons, we determined the organization of the microtubule and neurofilament cytoskeleton as a function of developmental age and F-actin depletion. Overall, the organization of microtubules and neurofilaments was similar in E7 and E14 axons and growth cones. Microtubules extended into the peripheral domain of both E7 and E14 growth cones on laminin and polylysine alike (Fig. 3). Similarly, immunocytochemistry for NF-M did not reveal obvious differences between E7 and E14 axons (Fig. 3). Neurofilament staining was present throughout the axon and did not extend as far into the growth cone as microtubule staining.

Chronic depletion of F-actin had different effects on the microtubule and neurofilament cytoskeleton of E7 and E14 axons. The axons of E14 CD-treated neurons contained a uniform array of microtubules and NF-M similar to that of DMSO-treated E14 controls (Fig. 3). In contrast, the E7 axons that were retained 24 h after F-actin depletion exhibited sparse neurofilaments and poorly bundled microtubules (Fig. 3), on both laminin and polylysine. Thus, chronic F-actin depletion disrupts the organization of the microtubule and neurofilament cytoskeleton in E7 but not in E14 axons.

Inhibition of Microtubule Dynamic Instability Blocks E14 Axon Extension in the Absence of F-Actin

Microtubules are required for axon extension (Dent and Gertler, 2003). However, the role of microtubules in driving axon extension in the absence of F-actin is not clear. Microtubules could drive axon extension in the absence of F-actin through two separate, and not mutually exclusive, mechanisms: dynamic instability of microtubule tips and/or transport of assembled microtubule polymer (Baas, 2002). Microtubule dynamic instability refers to repeated cycles of microtubule tip polymerization followed by depolymerization (Mitchison and Kirschner, 1984). To experimentally dissect the contributions of microtubule dynamic instability and transport to axon extension in the absence of F-actin, we used an established pharmacological regime that differentiates between these two mechanisms (Ahmad and Baas, 1995; Gallo and Letourneau, 1999). Low nanomolar concentrations of the microtubule drug VB prevent microtubule dynamic instability without causing depolymerization or altering transport. Therefore, we treated E14 DRG cultures on polylysine depleted of F-actin by CD treatment for 24 h with 0.5–1.0 n*M* VB and determined axon extension rates relative to vehicle-treated (DMSO) controls during the first hour of treatment. VB at 1.0 n*M* stopped axon extension [Fig. 4(A)], and did not cause axon retraction. VB at 0.5 n*M* inhibited the rate of axon extension by 50% relative to controls [Fig. 4(A)]. To confirm that these low concentrations of VB did not result in microtubule depolymerization, we determined the total amount of microtubule polymer in the distal 20 μm of axons. Cultures were simultaneously fixed and extracted, to remove soluble tubulin and retain the polymeric form reflective of microtubules (Gallo and Letourneau, 1999), and stained with anti-tubulin antibodies. A 1-h treatment with 1.0 n*M* VB did not decrease the amount of microtubule polymer, demonstrating that at these concentrations

VB did not result in depolymerization [Fig. 4(B)]. Thus, inhibition of microtubule dynamic instability using 1.0 n*M* VB completely stops axon extension in the absence of F-actin.

We have previously reported that in the absence of microtubule dynamic instability microtubules undergo transport and accumulate distally in collateral branches of DRG neurons over the course of 2–3 h (Gallo and Letourneau, 1999). Similarly, microtubules transported from the centrosome accumulate at the periphery of the soma and into the base of the axon (Ahmad et al., 1998). Therefore, we reasoned that if microtubule transport was not affected by VB we should detect an increase in microtubule polymer mass in the distal axons during prolonged VB treatment. Even after 2 h of treatment with 1.0 n*M* VB, CD-treated axons neither extended nor retracted (not shown). Quantification of total microtubule levels in the distal axons revealed a 62% increase in axons treated with VB for 2 h relative to DMSO-treated controls [Fig. 4(B)]. Thus, these observations confirm that VB did not cause microtubule depolymerization and did not interfere with the transport mechanism. Collectively these data demonstrate that microtubule dynamic instability is required for axon extension in the absence of F-actin, and that microtubule transport is not sufficient to maintain axon extension under these conditions.

E14 Axons Contain Decreased Levels of Tyrosinated Tubulin Relative to E7 Axons

Axon extension by E14 axons depleted of F-actin requires microtubule dynamic instability. This observation suggests that microtubule dynamics may differ as a function of developmental age and thus contribute differently to the ability of axons to extend following F-actin depletion. To determine whether net microtubule dynamics are altered as a function of developmental age, we investigated the relative levels of tyrosinated tubulin in E7 and E14 axons. Tubulin is posttranslationally modified as a function of time following polymerization into microtubules (Westermann and Weber, 2003). When α-tubulin subunits are incorporated into a microtubule tip they contain a C-terminus tyrosine residue. Following polymerization into microtubule tips, tubulin is detyrosinated as a function of time. Thus, more dynamic microtubule tips will exhibit increased levels of tyrosinated tubulin relative to total tubulin than more quiescent tips. Cultures were stained with antibodies to total tubulin and anti-tyrosinated tubulin and the ratio of tyrosinated tubulin to total tubulin in the distal 20 μm of axons was determined. The ratio of tyrosinated tubulin to total tubulin was decreased by 33% in E14 axons relative to E7 axons ($p < 0.04$) [Fig. 5(A,B)]. These data indicate that microtubules in E14 distal axons exhibit decreased net dynamic instability relative to E7 axons.

Microtubule Stability does not vary as a Function of Developmental Age

Although the tips of microtubules undergo dynamic instability, the shafts of microtubules are stable and do not undergo cycles of polymerization and depolymerization. Microtubule shaft stability is crucial to the maintenance of axonal morphology and depolymerization of microtubules causes axon disruption (Dent and Gertler, 2003). Tubulin acetylation is an additional time- and polymerization-dependent posttranslational modification of tubulin (Westermann and Weber, 2003). Dynamic microtubule tips exhibit decreased levels of tubulin acetylation relative to the main shaft. Thus, increased tubulin acetylation correlates with increased shaft microtubule stability. Ratiometric determination of the content of acetylated tubulin relative to total tubulin in the distal 40 μm of axons did not reveal a difference between E7 and E14 axons [Fig. 5(C)]. These data indicate that microtubule stability is not altered as a function of developmental age. Thus, while microtubule tip dynamic instability decreases with age, the stability of microtubules along their length does not change.

To confirm the lack of differential microtubule stability in E7 and E14 axons, we performed an additional stability assay. More stable microtubules undergo slower depolymerization in response to pharmacological inhibitors of polymerization (Baas and Black, 1990). In

preliminary studies, we determined a concentration of VB (6 n*M*) that resulted in approximately 50% depolymerization of E7 microtubules in the distal 40 μm of axons during a 20-min treatment period. Subsequently, both E14 and E7 cultures were treated with either 6 n*M* VB or DMSO as a control. Treatment with 6 n*M* VB for 20 min resulted in a 48 and 40% decrease in the microtubule content of E7 and E14 axons, respectively [Fig. 5(D)]. Statistical comparison of the normalized decrease in microtubule mass as a function of VB treatment in E7 and E14 axons did not reveal a statistically significant difference [Fig. 5(D)]. Furthermore total microtubule mass in axons did not vary as a function of developmental age [$p > 0.4$, determined from the control axons quantified in Fig. 5(D)]. Collectively, measurements of acetylated tubulin levels [Fig. 5(C)] and the experimental depolymerization of microtubules using high doses of VB [Fig. 5(D)] demonstrate that axonal microtubule stability does not differ as a function of developmental age and thus is not likely to contribute to the differences in axon extension and maintenance in F-actin depleted E7 and E14 axons.

E14 Axons are More Sensitive than E7 Axons to Inhibition of Microtubule Dynamic Instability

The observation that E14 axons exhibit decreased net microtubule dynamics relative to E7 axons suggests that the extension of E14 axons may be more dependent on microtubule dynamics. Therefore, we next sought to test whether the extension rates of E7 and E14 axons exhibit differential sensitivity to inhibition of microtubule dynamic instability using VB. Cultures were treated with 0.5–1 n*M* VB and axon extension rates were monitored prior to and following the addition of VB. These experiments revealed that E7 axon extension is inhibited by 51% following treatment with 1 n*M* VB [Fig. 5(E)]. However, 1 n*M* VB treatment decreased the extension rate of E14 axons by 84% [Fig. 5(E)]. VB (0.5 n*M*) had similar effects on the rate of axon extension on both E7 and E14 axons (data not shown). However, comparison of the effects of 0.5 and 1.0 n*M* VB on axon extension rate within age group revealed that 1.0 n*M* further decreased the rate in E14 ($p < 0.05$) but not E7 axons ($p > 0.8$). These data indicate that the extension of E14 axons is more sensitive to inhibition of microtubule dynamic instability than the extension of E7 axons. Thus, relative to E7 axons, the extension of E14 axons is less dependent on F-actin but more dependent on microtubule dynamic instability.

Live Imaging of Microtubule Tip Polymerization in E7 and E14 Axons

The previous data indicate that microtubule dynamics in E14 axons are dampened relative to E7, but provide a greater contribution to axon extension rate. In order to directly determine the dynamics of polymerizing microtubule tips in distal axons, we transfected dissociated DRG neurons with EGFP-EB3. EB3 is a protein that associates selectively with the tips of polymerizing microtubules and is released when the tip undergoes depolymerization (Stepanova et al., 2003). The utility and reliability of the EB3-reporter system for imaging microtubule tip polymerization has been further confirmed by Ma et al. (2004). Thus, EGFP-EB3 is an ideal tool for imaging the tips of microtubules in regions of the axon where the background from total tubulin precludes detection of single tips using fluorescently labeled tubulin. The majority of microtubules in axons are polarized with the rapidly polymerizing plus end directed toward the growth cone. We focused our analysis on anterogradely advancing EB3 comets and did not include the small percentage of retrogradely directed comets (Stepanova et al., 2003; Ma et al., 2004; unpublished observations). Dynamic instability consists of periods of microtubule tip polymerization followed by rapid depolymerization. The transition from polymerization to depolymerization is termed a “catastrophe.” Thus, EB3 comets reveal the polymerization phase of dynamic instability and their lifespan reports on the time between initiation of tip polymerization and a catastrophe. Tanaka and Kirschner (1991) report that only 15% of neuronal microtubules enter brief quiescent states, neither polymerizing nor extending, indicating that when not actively polymerizing the majority of microtubule tips undergo depolymerization. Quantification of comet lifespans determined that E14 microtubule tips polymerized for 25% less time than E7 [Fig. 6(A and B)]. In addition,

quantification of the advance rate of EB3 comets revealed a 40% decrease in E14 axons relative to E7 axons [Fig. 6(C)]. Exemplary timelapse video sequences of EB3-GFP in the axons of E7 and E14 are provided in the supplementary materials (Movie 1S and 2S, respectively).

The live analysis of microtubule tip polymerization is consistent with decreased levels of tyrosinated tubulin in E14 relative to E7 axons. The decreases in EB3 comet lifespan in E14 axons suggest that microtubule tips underwent more frequent catastrophes in E14 than E17 axons. Moreover, the rate of tip polymerization was also decreased. Thus, E14 microtubule tips exhibit a different pattern of dynamic instability relative to E7 axons that is also revealed by decreased tyrosinated tubulin levels indicating decreased net dynamic instability.

DISCUSSION

Elucidating developmental changes in neurons is of fundamental importance to understanding the development and regenerative potential of the nervous system. Current models for the lack of robust regeneration in the adult nervous system emphasize the importance of myelin-derived inhibitory signals that collapse growth cones (Domeniconi and Filbin, 2005). However, this growth cone collapsing activity is determined in embryonic neurons grown in culture and it is by no means certain that axons regenerating in the mature nervous system have growth cones. Furthermore, a growing body of evidence indicates that a major contribution to the failure of axon regeneration is due to cell intrinsic developmental changes independent of myelination (Chen et al., 1995; Li et al., 1995; Dusart et al., 1997; Udvadia et al., 2001; Goldberg et al., 2002; Bouslama-Oueghlani et al., 2003; Dusart et al., 2005; Blackmore and Letourneau, 2006). Previous work identified age-dependent differences in the pattern of axon extension (Bray et al., 1987) and determined that these changes correlate with the ability of axons to regenerate in vivo (Smith and Skene, 1997; Bomze et al., 2001). Changes in the expression of CAP-23 and GAP-43, regulators of F-actin dynamics and organization in growth cones, have also been shown to contribute to differences in the pattern of axon extension and regenerative potential (Bomze et al., 2001). A developmental decrease in cAMP levels alters the response of neurons to myelin-derived inhibitory signals (Spencer and Filbin, 2004). Similarly, differences have been uncovered in the signaling pathways that support axon extension from developing embryonic and regenerating adult mouse sensory neurons (Liu and Snider, 2001). Thus, it is becoming increasingly clear that neurons undergo developmental changes that regulate the mechanism of axon extension and elucidating these changes may have important implications for the rational design of therapies aimed at promoting axon regeneration in the injured mature nervous system.

In this study we used an *in vitro* model system to address the question of whether embryonic sensory axons undergo a developmental change in the dynamics of the cytoskeleton underlying axon regeneration. In relation to the mechanism of axon regeneration *in vivo*, several caveats apply to our results. First, although axons in our *in vitro* system were previously axotomized, and thus regenerating, the environment the axons regenerated within is clearly different from the *in vivo* environment, which includes a variety of positive and inhibitory extracellular signals not present in our culturing system (Selzer, 2003; Domeniconi and Filbin, 2005). Second, growth cones and axons may be responding in a developmentally regulated manner to some aspect of the culturing environment. Despite these caveats, the present study identifies a developmentally regulated difference in the ability of sensory axons to regenerate under defined and constant conditions, indicating a cell intrinsic developmental difference. Future studies will be required to determine if a similar developmentally regulated change in the ability of sensory axons to regenerate in the absence of F-actin operates *in vivo*. Furthermore, additional studies of changes in growth cone structure and cytoskeletal organization *in vivo* will greatly expand our current knowledge. At the present time, such studies are limited to the

regeneration of axons following spinal cord transection in the lamprey (Lurie et al., 1994; Hall et al., 1997; Zhang et al., 2005).

Embryonic Sensory Axon Extension Rate is not Determined by Growth Cone Complexity or F-Actin Levels

Major emphasis is placed on the growth cone as a fundamental structure mediating axon extension and guidance (Dent and Gertler, 2003). Previous reports identified developmental decreases in axon extension rate between cultured embryonic and postembryonic sympathetic neurons that correlated with smaller growth cone sizes and decreased lamellipodial surface area (Argiro and Johnson, 1982; Argiro et al., 1984; Kleitman and Johnson, 1989). In contrast to these previous reports, we report that the complexity of growth cone morphology and F-actin content are not by necessity related to the rate of axon extension. Differences in the developmental time windows studied, two embryonic ages (our study) and embryonic relative to postnatal in previous studies, may underlie the discrepancy between previous studies and our results. Alternatively, the differences in the neuronal model system used might also explain this discrepancy.

Developmentally, early (E7) DRG axons exhibit complex growth cones containing relatively large amounts of F-actin, but extend at similar rates as developmentally older (E14) axons that exhibit smaller growth cones with significantly decreased F-actin content. Furthermore, E7 axons exhibit a strict dependence on F-actin for maintenance and extension while E14 axons continue to extend in the absence of F-actin, albeit at decreased rates relative to age-matched controls with normal levels of F-actin. These observations indicate that the dependence of axon maintenance and extension on F-actin changes during development in a manner proportional to the endogenous levels of growth cone F-actin. Whether at later developmental stages axon extension becomes more independent of F-actin is not known. Regenerating reticulospinal axons in the lamprey spinal cord appear to extend without growth cones or F-actin accumulation at their tips (Lurie et al., 1994; Zhang et al., 2005). However the tips of these regenerating axons contain microtubules and neurofilaments. Thus, it has been proposed that in regeneration, as opposed to early development, axon extension may be based on internal protrusive forces due to either the transport or polymerization of neurofilaments or microtubules. The present results are consistent with microtubule tip polymerization providing a major contribution to the rate of extension of regenerating axons depleted of F-actin, either experimentally or by developmental decreases in the amount of F-actin in growth cones. It remains to be determined if the changes in growth cone F-actin levels are due to decreased levels of actin protein expression, or differences in the relative polymerization of actin without concurrent changes in actin protein levels.

Developmental Regulation of the Requirement of F-Actin for Maintenance of the Axonal Cytoskeleton

The organization of neurofilaments in E7, but not E14, axons was severely disrupted by chronic F-actin depolymerization. The disruption of neurofilament organization may be reflective of altered neurofilament axonal transport. Jung et al. (2004) have reported that F-actin is required for the axonal transport of neurofilaments in NB2a/d1 cells induced into a neuronal phenotype. In contrast, Francis et al. (2005) reported that actin filaments are not required for neurofilament transport in superior cervical ganglia neurons obtained from postnatal rat pups. The discrepancy between the results of Jung et al. (2004) and Francis et al. (2005) may reflect the cell model system used. NB2a/d1 cells are induced to become neuron-like *in vitro* (Jung et al., 2004) and thus may represent an early stage in neuronal differentiation, perhaps analogous to E7 DRG neurons, while postnatal neurons clearly represent well differentiated neurons (Francis et al., 2005). Thus, the disruption of E7 axon maintenance and lack of continued extension following F-actin depolymerization may be due to developmental stage specific

functions for F-actin in regulating the transport of neurofilaments, and possibly microtubules (Hasaka et al., 2004). This issue will require additional investigation. Regardless, the present data demonstrate significant differences in the requirement of F-actin for the maintenance of axons in a developmentally regulated manner.

E14 Axon Extension in the Absence of F-Actin Requires Microtubule Tip Polymerization

Our data demonstrate that microtubule tip dynamic instability is required for axon extension by E14 neurons in the absence of F-actin. Vinblastine at 1.0 n*M* completely stopped axon extension by inhibiting microtubule dynamic instability without preventing transport or depolymerizing microtubules. These observations have multiple implications. First, since at least in the lamprey, axon regeneration appears to occur by a mechanism that is independent of F-actin and growth cones (Lurie et al., 1994; Hall et al., 1997; Zhang et al., 2005), microtubule dynamic instability may be an important parameter to regulate during attempts at increasing axon extension rates. Indeed, Grenningloh et al. (2004) report that overexpression of stathmin, a protein that increases the frequency of microtubule tip catastrophes, increases axon extension. In addition, proteins that regulate microtubule tip dynamics are up regulated during regeneration (Iwata et al., 2002). Second, our results are conceptually consistent with the "push" and "pull" model of axon extension (Letourneau et al., 1987). In this model actin filaments, and presumably myosin based contractile forces, provide the "pulling" force, and microtubules provide the "pushing" force. Janson et al. (2003) determined the polymerization of a single microtubule tip generates forces in the piconewton range. Goldberg and Burmeister (1992) demonstrated that microtubules produce sufficient force to generate protrusions from the severed ends of axons in the absence of actin filaments. Forces generated by microtubule tip polymerization may in turn be able to overcome intrinsic membrane tension and allow the axon to extend (Raucher and Sheetz, 2000). Thus the polymerizing microtubule tips present in the tips of E14 F-actin depleted axons may produce sufficient force to "push" the axon tip forward resulting in extension. Our data suggest that if microtubule tips are providing the "push", then the pattern of decreased dynamic instability exhibited by E14 axons positively contributes to the "pushing" force. Whether microtubule polymerization underlies the regeneration of lamprey spinal cord axons, or axons in other species, remains to be determined.

Developmental Regulation of Microtubule Tip Dynamic Instability

Our studies identify developmental changes in the dynamic instability of axonal microtubule tips in the absence of altered net microtubule stability. Importantly, the extension rate of E14 axons is more sensitive to inhibition of microtubule dynamic instability than E7 axons. While the mechanistic interpretation of altered dynamic instability at microtubule tips *vis-a-vis* the ability of E14 axons to extend in the absence of F-actin is currently not clear, the requirement for dynamic instability indicates that these changes have functional significance. Dynamic instability contributes to normal axon extension through regulation of the F-actin cytoskeleton (Rodriguez et al., 2003). However, regulation of F-actin cannot be the basis for the requirement of dynamic instability in F-actin depleted axons. Dynamic instability has also been shown to drive membrane insertion in growth cones (Zakharenko and Popov, 1998). This observation suggests that older axons may exhibit differences in the delivery of membrane and organelles thereby allowing for axon extension in the absence or lowered levels of growth cone F-actin. Thus, in addition to differential contributions to microtubule based "pushing" of the axon, the differences in microtubule dynamic instability between E7 and E14 axons may also be reflected in altered membrane insertion. These issues will require further investigation.

The rate of microtubule tip polymerization in E14 axons (0.13 μm/s) is sixfold greater than that of axon extension (0.02 μm/s). Thus, although microtubule polymerization is attenuated in E14 axons relative to E7 axons, the decrease in polymerization rate is not expected to negatively affect axon extension rate. This consideration further indicates that changes in the

dynamic instability of microtubules underlie the age-dependent changes in the requirement for microtubule dynamics in regulating axon extension rate.

CONCLUSIONS

Our results suggest the hypothesis that there are two mechanisms of axon extension with varying dependence on F-actin. This hypothesis is supported by a study investigating the effects of F-actin depletion on axon extension relative to the culturing substratum (Abosch and Lagenaur, 1993). These authors report that axon extension by cerebellar neurons was not inhibited by F-actin depletion on L1. However, F-actin depletion partially inhibited axon extension on laminin, and completely blocked it on N-CAM. Interestingly, in the study by Abosch and Lagenaur (1993) growth cones grown on N-CAM were characterized by F-actin-rich lamellipodia and exhibited the most complex morphology relative to the other substrata. Conversely, growth cones on L1 were small and predominantly filopodial. Thus, cerebellar growth cones on L1 and N-CAM appear analogous to E7 and E14 DRG growth cones on laminin or polylysine, in terms of their F-actin content and sensitivity to F-actin depletion. The dependence of axon extension on F-actin in our investigation and that by Abosch and Lagenaur (1993) correlates with the degree of growth cone F-actin content, indicating that the F-actin-dependent mechanism of axon extension promotes F-actin polymerization in the growth cone. Furthermore, collectively our study and that of Abosch and Lagenaur (1993) indicate that the two mechanisms can be tapped into by either developmental age or substratum-mediated signaling.

In conclusion, the present study identifies developmental changes in microtubule dynamic instability that may compensate for changes in growth cone F-actin content, thereby allowing axons to extend in conditions of F-actin depletion. In future work it will be of interest to determine the molecular basis of the switch from a strictly F-actin-dependent mode of axon maintenance and extension in E7 axons to the partially F-actin-independent mode exemplified by E14 axon extension in the absence of F-actin. In addition, our data indicate that the developmental age of the neuron must be taken into consideration when comparing and designing experiments on the mechanisms of axon extension. Finally, these observations indicate that care must be taken in the extrapolation of information obtained from studies of the cytoskeletal basis of axon extension in early embryonic neurons to the mechanism of axon extension underlying the regeneration of more mature axons.

Supplementary Material

Refer to Web version on PubMed Central for supplementary material.

Acknowledgements

Contract grant sponsor: NIH; contract grant numbers: NS043251, NS048090, NS14837, NS38537.

Contract grant sponsor: PVA/SCRF; contract grant number: 2199-01.

The authors thank Mr. Benjamin Keeler (Drexel University) for technical assistance.

REFERENCES

Abosch A, Lagenaur C. Sensitivity of neurite outgrowth to microfilament disruption varies with adhesion molecule substrate. J Neurobiol 1993;24:344–355.

Ahmad FJ, Baas PW. Microtubules released from the neuronal centrosome are transported into the axon. J Cell Sci 1995;108:2761–2769. [PubMed: 7593317]

Ahmad FJ, Echeverri CJ, Vallee RB, Baas PW. Cytoplasmic dynein and dynactin are required for the transport of microtubules into the axon. J Cell Biol 1998;140:391–401. [PubMed: 9442114]

Argiro V, Bunge MB, Johnson MI. Correlation between growth form and movement and their dependence on neuronal age. J Neurosci 1984;4:3051–3062. [PubMed: 6502223]

Argiro V, Johnson MI. Patterns and kinetics of neurite extension from sympathetic neurons in culture are age dependent. J Neurosci 1982;2:503–512. [PubMed: 7069468]

Baas PW. Microtubule transport in the axon. Int Rev Cytol 2002;212:41–62. [PubMed: 11804039]

Baas PW, Black MM. Individual microtubules in the axon consist of domains that differ in both composition and stability. J Cell Biol 1990;111:495–509. [PubMed: 2199458]

Blackmore M, Letourneau PC. Changes within maturing neurons limit axonal regeneration in the developing spinal cord. J Neurobiol 2006;66:348–360. [PubMed: 16408302]

Bomze HM, Bulsara KR, Iskandar BJ, Caroni P, Skene JH. Spinal axon regeneration evoked by replacing two growth cone proteins in adult neurons. Nat Neurosci 2001;4:38–43. [PubMed: 11135643]

Bouslama-Oueghlani L, Wehrle R, Sotelo C, Dusart I. The developmental loss of the ability of Purkinje cells to regenerate their axons occurs in the absence of myelin: An in vitro model to prevent myelination. J Neurosci 2003;23:8318–8329. [PubMed: 12967994]

Bradke F, Dotti CG. The role of local actin instability in axon formation. Science 1999;283:1931–1934. [PubMed: 10082468]

Bray D, Bunge MB, Chapman K. Geometry of isolated sensory neurons in culture. Effects of embryonic age and culture substratum. Exp Cell Res 1987;168:127–137. [PubMed: 3780869]

Carr VM, Simpson SB Jr. Proliferative and degenerative events in the early development of chick dorsal root ganglia. I. Normal development. J Comp Neurol 1978;182:727–739. [PubMed: 721975]

Chen DF, Jhaveri S, Schneider GE. Intrinsic changes in developing retinal neurons result in regenerative failure of their axons. Proc Natl Acad Sci USA 1995;92:7287–7291. [PubMed: 7638182]

Coue M, Brenner SL, Spector I, Korn ED. Inhibition of actin polymerization by latrunculin A. FEBS Lett 1987;213:316–318. [PubMed: 3556584]

Dent EW, Gertler FB. Cytoskeletal dynamics and transport in growth cone motility and axon guidance. Neuron 2003;40:209–227. [PubMed: 14556705]

Domeniconi M, Filbin MT. Overcoming inhibitors in myelin to promote axonal regeneration. J Neurol Sci 2005;233:43–47. [PubMed: 15949495]

Dusart I, Airaksinen MS, Sotelo C. Purkinje cell survival and axonal regeneration are age dependent: An in vitro study. J Neurosci 1997;17:3710–3726. [PubMed: 9133392]

Dusart I, Ghoumari A, Wehrle R, Morel MP, Bouslama-Oueghlani L, Camand E, Sotelo C. Cell death and axon regeneration of Purkinje cells after axotomy: Challenges of classical hypotheses of axon regeneration. Brain Res Brain Res Rev 2005;49:300–316. [PubMed: 16111558]

Emery DL, Royo NC, Fischer I, Saatman KE, McIntosh TK. Plasticity following injury to the adult central nervous system: Is recapitulation of a developmental state worth promoting? J Neurotrauma 2003;20:1271–1292. [PubMed: 14748977]

Ernst AF, Gallo G, Letourneau P, McLoon SC. Stabilization of growing retinal axons by the combined signaling of nitric oxide and brain-derived neurotrophic factor. J Neurosci 2000;20:1458–1469. [PubMed: 10662836]

Francis F, Roy S, Brady ST, Black MM. Transport of neurofilaments in growing axons requires microtubules but not actin filaments. J Neurosci Res 2005;79:442–450. [PubMed: 15635594]

Gallo G, Letourneau PC. Different contributions of microtubule dynamics and transport to the growth of axons and collateral sprouts. J Neurosci 1999;19:3860–3873. [PubMed: 10234018]

Gallo G, Letourneau PC. Regulation of growth cone actin filaments by guidance cues. J Neurobiol 2004;58:92–102. [PubMed: 14598373]

Goldberg DJ, Burmeister DW. Microtubule-based filopodium-like protrusions form after axotomy. J Neurosci 1992;12:4800–4807. [PubMed: 1464768]

Goldberg JL, Klassen MP, Hua Y, Barres BA. Amacrine-signaled loss of intrinsic axon growth ability by retinal ganglion cells. Science 2002;296:1860–1864. [PubMed: 12052959]

Gorgels TG. Outgrowth of the pyramidal tract in the rat cervical spinal cord: Growth cone ultrastructure and guidance. J Comp Neurol 1991;306:95–116. [PubMed: 2040732]

Grenningloh G, Soehrman S, Bondallaz P, Ruchti E, Cadas H. Role of the microtubule destabilizing proteins SCG10 and stathmin in neuronal growth. J Neurobiol 2004;58:60–69. [PubMed: 14598370]

Guan W, Puthenveedu MA, Condic ML. Sensory neuron subtypes have unique substratum preference and receptor expression before target innervation. J Neurosci 2003;23:1781–1791. [PubMed: 12629182]

Hall GF, Yao J, Selzer ME, Kosik KS. Cytoskeletal changes correlated with the loss of neuronal polarity in axotomized lamprey central neurons. J Neurocytol 1997;26:733–753. [PubMed: 9426171]

Hasaka TP, Myers KA, Baas PW. Role of actin filaments in the axonal transport of microtubules. J Neurosci 2004;24:11291–11301. [PubMed: 15601935]

Iwata T, Namikawa K, Honma M, Mori N, Yachiku S, Kiyama H. Increased expression of mRNAs for microtubule disassembly molecules during nerve regeneration. Brain Res Mol Brain Res 2002;102:105–109. [PubMed: 12191499]

Janson ME, de Dood ME, Dogterom M. Dynamic instability of microtubules is regulated by force. J Cell Biol 2003;161:1029–1034. [PubMed: 12821641]

Jung C, Chylinski TM, Pimenta A, Ortiz D, Shea TB. Neurofilament transport is dependent on actin and myosin. J Neurosci 2004;24:9486–9496. [PubMed: 15509735]

Kleitman N, Johnson MI. Rapid growth cone translocation on laminin is supported by lamellipodial not filopodial structures. Cell Motil Cytoskeleton 1989;13:288–300. [PubMed: 2776225]

Kuhn TB, Brown MD, Bamburg JR. Rac1-dependent actin filament organization in growth cones is necessary for β1-integrin-mediated advance but not for growth on poly-D-lysine. J Neurobiol 1998;37:524–540. [PubMed: 9858256]

Lelkes, PI.; Unsworth, BR.; Saporta, S.; Cameron, DF.; Gallo, G. Culture of neuroendocrine and neuronal cells for tissue engineering. In: Vunjak-Novakovic, G.; Freshney, RI., editors. Culture of Cells for Tissue Engineering. Wiley; New York: 2006. Chapter 14

Letourneau PC, Shattuck TA, Ressler AH. “Pull” and “push” in neurite elongation: Observations on the effects of different concentrations of cytochalasin B and taxol. Cell Motil Cytoskeleton 1987;8:193–209. [PubMed: 2891448]

Li D, Field PM, Raisman G. Failure of axon regeneration in postnatal rat entorhinohippocampal slice coculture is due to maturation of the axon, not that of the pathway or target. Eur J Neurosci 1995;7:1164–1171. [PubMed: 7582089]

Liu RY, Snider WD. Different signaling pathways mediate regenerative versus developmental sensory axon growth. J Neurosci 2001;21:RC164. [PubMed: 11511695]

Lurie DI, Pijak DS, Selzer ME. Structure of reticulospinal axon growth cones and their cellular environment during regeneration in the lamprey spinal cord. J Comp Neurol 1994;344:559–580. [PubMed: 7929892]

Ma Y, Shakiryanova D, Vardya I, Popov SV. Quantitative analysis of microtubule transport in growing nerve processes. Curr Biol 2004;14:725–730. [PubMed: 15084289]

Marsh L, Letourneau PC. Growth of neurites without filopodial or lamellipodial activity in the presence of cytochalasin B. J Cell Biol 1984;99:2041–2047. [PubMed: 6389568]

Mason CA. Growing tips of embryonic cerebellar axons in vivo. J Neurosci Res 1985;13:55–73. [PubMed: 4038747]

Mitchison T, Kirschner M. Dynamic instability of microtubule growth. Nature 1984;312:237–242. [PubMed: 6504138]

Nordlander RH. Axonal growth cones in the developing amphibian spinal cord. J Comp Neurol 1987;263:485–496. [PubMed: 3667985]

Raucher D, Sheetz MP. Cell spreading and lamellipodial extension rate is regulated by membrane tension. J Cell Biol 2000;148:127–136. [PubMed: 10629223]

Rodriguez OC, Schaefer AW, Mandato CA, Forscher P, Bement WM, Waterman-Storer CM. Conserved microtubule—actin interactions in cell movement and morphogenesis. Nat Cell Biol 2003;5:599–609. [PubMed: 12833063]

Ruthel G, Hollenbeck PJ. Growth cones are not required for initial establishment of polarity or differential axon branch growth in cultured hippocampal neurons. J Neurosci 2000;20:2266–2274. [PubMed: 10704502]

Selzer ME. Promotion of axonal regeneration in the injured CNS. Lancet Neurol 2003;2:157–166. [PubMed: 12849237]

Smith DS, Skene JH. A transcription-dependent switch controls competence of adult neurons for distinct modes of axon growth. J Neurosci 1997;17:646–658. [PubMed: 8987787]

Spector I, Shochet NR, Blasberger D, Kashman Y. Latrunculins—Novel marine macrolides that disrupt microfilament organization and affect cell growth. I. Comparison with cytochalasin D. Cell Motil Cytoskeleton 1989;13:127–144. [PubMed: 2776221]

Spencer T, Filbin MT. A role for cAMP in regeneration of the adult mammalian CNS. J Anat 2004;204:49–55. [PubMed: 14690477]

Stepanova T, Slemmer J, Hoogenraad CC, Lansbergen G, Dortland B, De Zeeuw CI, Grosveld F, et al. Visualization of microtubule growth in cultured neurons via the use of EB3—GFP (end-binding protein 3—green fluorescent protein). J Neurosci 2003;23:2655–2664. [PubMed: 12684451]

Tanaka EM, Kirschner MW. Microtubule behavior in the growth cones of living neurons during axon elongation. J Cell Biol 1991;115:345–363. [PubMed: 1918145]

Udvadia AJ, Koster RW, Skene JH. GAP-43 promoter elements in transgenic zebrafish reveal a difference in signals for axon growth during CNS development and regeneration. Development 2001;128:1175–1182. [PubMed: 11245583]

Westermann S, Weber K. Post-translational modifications regulate microtubule function. Nat Rev Mol Cell Biol 2003;4:938–947. [PubMed: 14685172]

Zakharenko S, Popov S. Dynamics of axonal microtubules regulate the topology of new membrane insertion into the growing neurites. J Cell Biol 1998;143:1077–1086. [PubMed: 9817763]

Zhang G, Jin L-Q, Selzer ME. Live imaging of regenerating lamprey spinal axons. Neurorehabil Neural Repair 2005;19:46–57. [PubMed: 15673843]

Zmuda JF, Rivas RJ. Actin filament disruption blocks cerebellar granule neurons at the unipolar stage of differentiation in vitro. J Neurobiol 2000;43:313–328. [PubMed: 10861558]

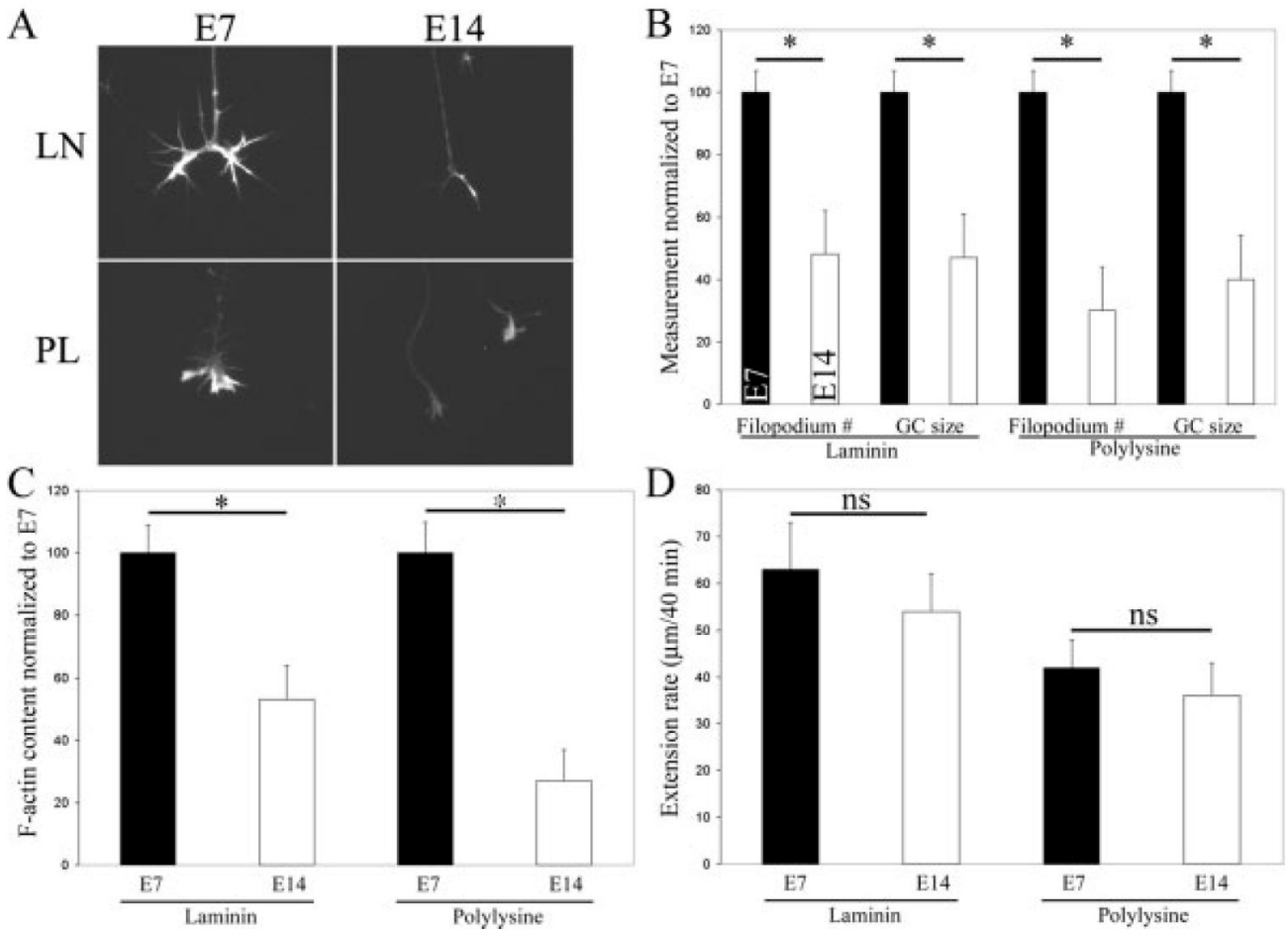

Figure 1.

Analysis of E7 and E14 growth cone morphology and F-actin content. (A) Representative examples of E7 and E14 growth cones on laminin- (LN) and polylysine- (PL) coated substrata. (B) Quantification of filopodium number and growth cone size (2 μm). Black bars represent E7 and white bars represent E14. (C) Quantification of the total F-actin content of E7 and E14 growth cones on LN and PL. For panels B and C, n = 46–49 growth cones per group. (D) Determination of axon extension rates from phase contrast videos of E7 and E14 axons extending on LN- or PL-coated substrata. n = 26–36 axons per group. *$p < 0.001$.

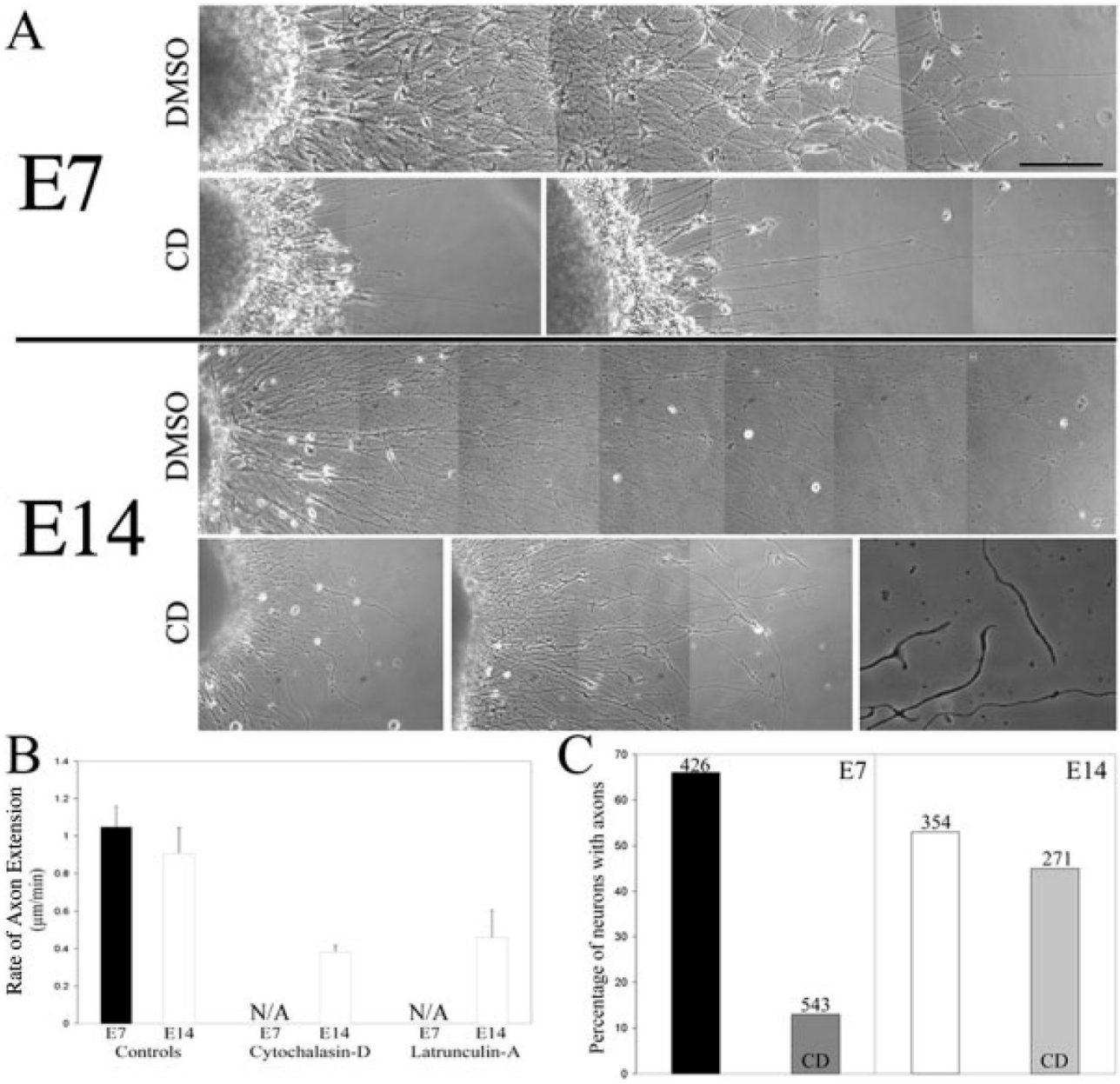

Figure 2.

Differential effects of F-actin depletion on E7 and E14 sensory axons. (A) Phase contrast montages of axons extending from DRG explants (on left). The DMSO panels show the appearance of axons treated for 24 h with DMSO starting at 24 h post plating. The CD panels show examples of axons treated for 24 h with 2 μg/mL cytochalasin D (CD) starting at 24 h post plating. Note that the E7 axons have largely retracted. The few E7 axons that remain appear thin. In contrast, although E14 axons have also undergone some degree of retraction, the axons seem relatively thick. The last panel of the E14 CD treated row shows the appearance of E14 axons at higher resolution. F-actin depletion using 2 μM latrunculin A or 166 n*M* swinholide A produced similar results (not shown). The described effects were present on both laminin (shown) and polylysine substrata (not shown; bar, 200 μm). (B) Determination of extension rate of control (DMSO treated) and F-actin depleted axons treated with 2 μg/mL cytochalasin

D 8 or 2 μM latrunculin A cultured on polylysine. Cultures were treated for 24 h with reagents at time of determination. We failed to observe E7 axons extend in cytochalasin D or latrunculin A treated cultures (NA, not applicable). E14 axons continued to extend, albeit at decreased rates ($p < 0.01$), in both cytochalasin D and latrunculin A treated cultures. $n = 26–40$ axons per group. (C) Determination of the percentage of neurons exhibiting axons in cultures of dissociated DRG neurons plated in the presence of CD and fixed 24 h later. Cultures were stained with antibodies specific to neuronal tubulin for determination of axon formation. Numbers on top of bars reflect the number of neurons sampled to obtain the percentage. Neurons were plated on substrata coated with polylysine and laminin. F-actin depletion decreased axon formation by 80% and 15% in E7 and E14 cultures, respectively.

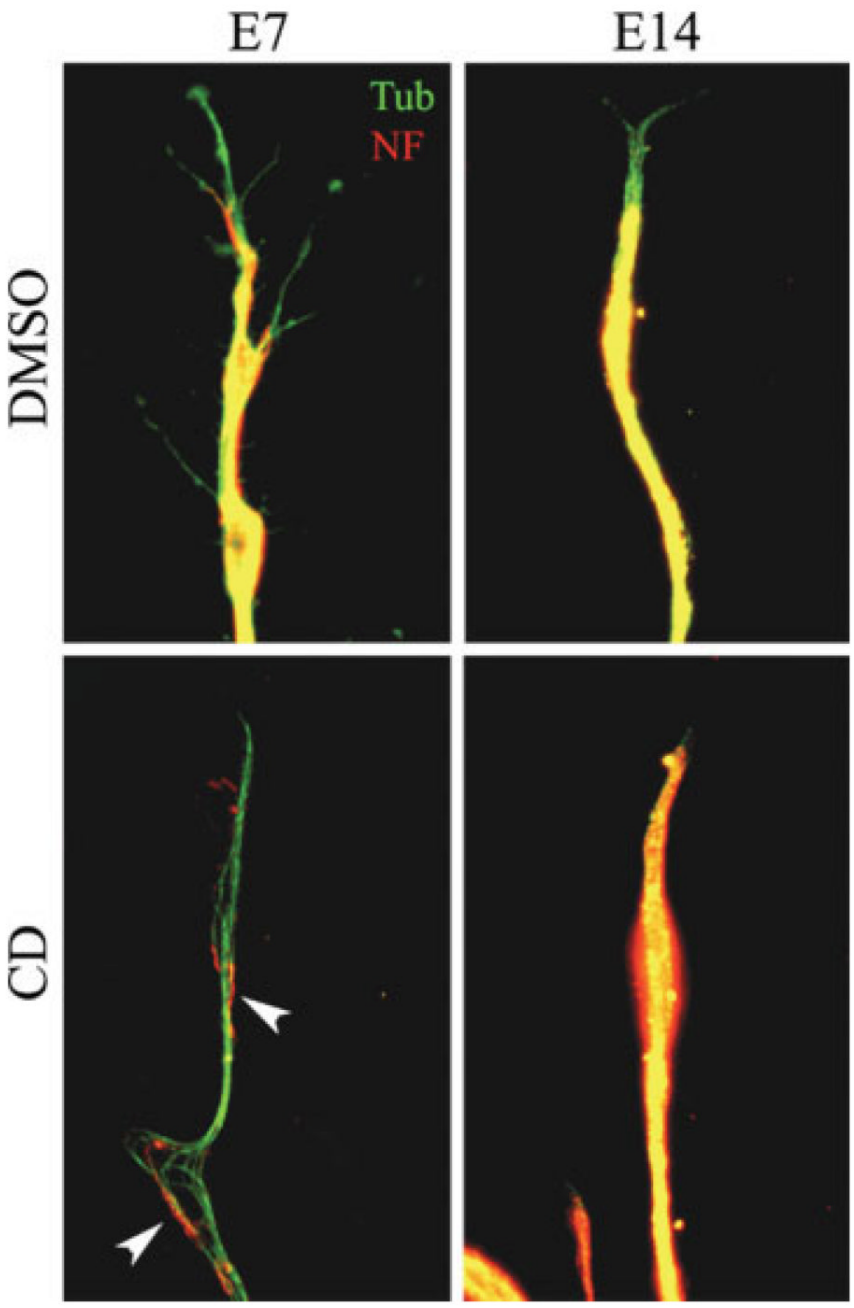

Figure 3.

Developmental age-dependent effects of F-actin depletion on axonal microtubule and neurofilament organization. DRG explants were cultured for 24 h on substrata coated with polylysine and laminin prior to treatment with latrunculin A or cytochalasin D (shown) for an additional 24 h. Following fixation cultures were stained with antibodies to tubulin (Tub) and neurofilament-M (NF). In both E7 and E14 control axons (DMSO) the neurofilament array was uniform, but did not extend as far distally as the microtubules. Following chronic F-actin depeletion E7 axons exhibited debundled microtubules and sparse neurofilaments (arrowheads). In contrast, E14 axons retained a uniform array of neurofilaments and microtubules. Microtubules were noted a few microns ahead of the neurofilament staining in

almost every control axon regardless of age. F-actin depleted E14 axons exhibited more overlap between neurofilament and microtubule staining at the tips of axons (compare DMSO and CD in E14 column). [Color figure can be viewed in the online issue, which is available at www.interscience.wiley.com.]

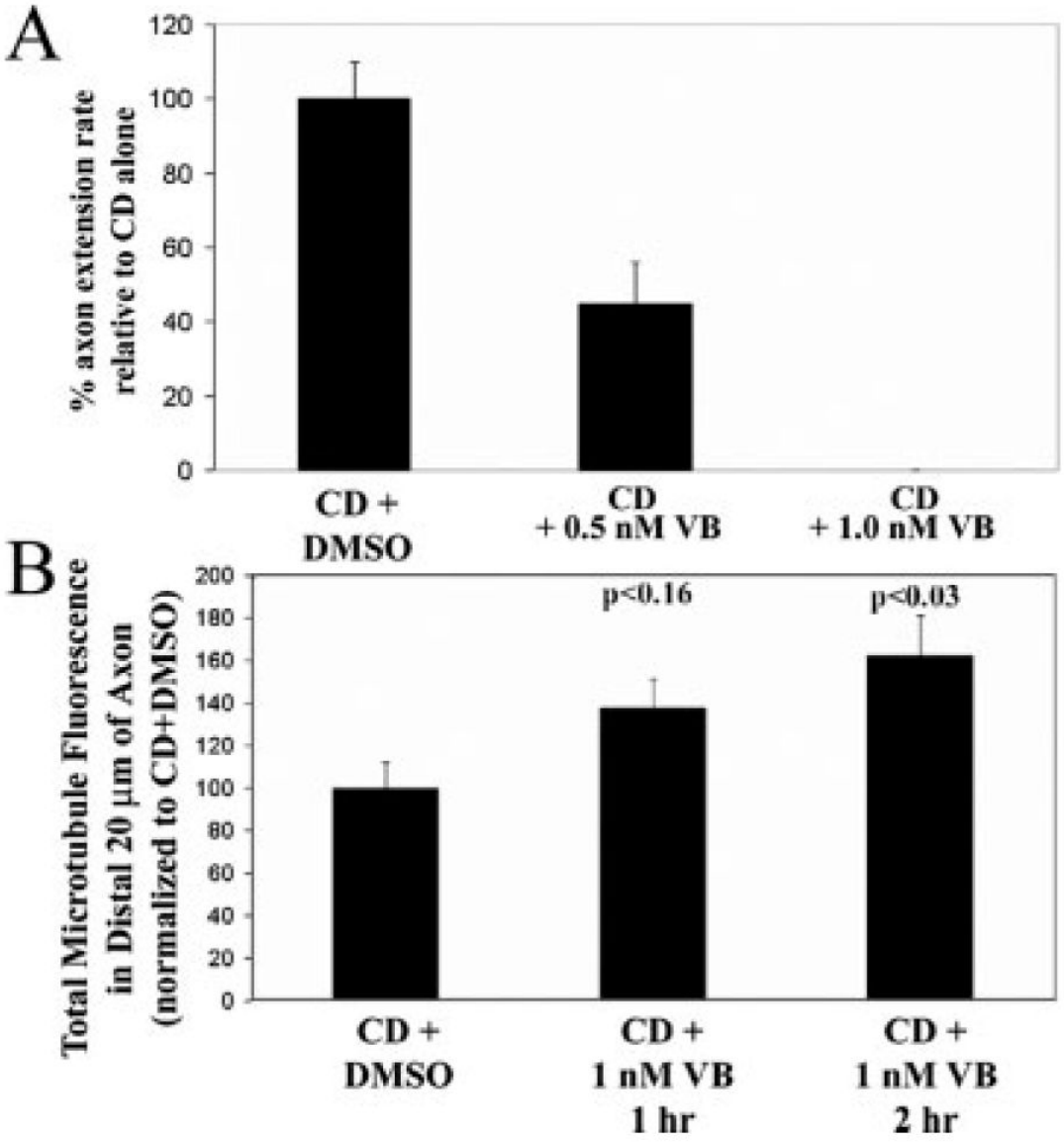

Figure 4.

Inhibition of microtubule dynamic instability blocks E14 axon extension in the absence of F-actin. (A) E14 DRG explant cultures were treated with 2 μ/mL cytochalasin D (CD) for 24 h starting at 24 h post plating (as in experiments in Figs. 2 and 3). Phase timelapse videos were then obtained of axons extending following DMSO or VB treatment. VB (0.5 n*M*) inhibited extension in the presence of CD by 50%. VB (1.0 n*M*) stopped extension in the presence of CD, and did not induce retraction. For this and all subsequent experiments neurons were cultured on polylysine. (B) Cultures were treated as in (A) and then simultaneously fixed and extracted and stained with antibodies to tubulin. The total amount of tubulin staining in the distal 20 μm of axons was then assessed. Cultures were treated with VB for 1 or 2 h prior to fixation. A 1-h treatment with VB increased microtubule mass in the distal axons by approximately 40%, but the *p* value did not reach significance. A 2 h VB treatment significantly increased microtubule mass in the distal axon by 62%.

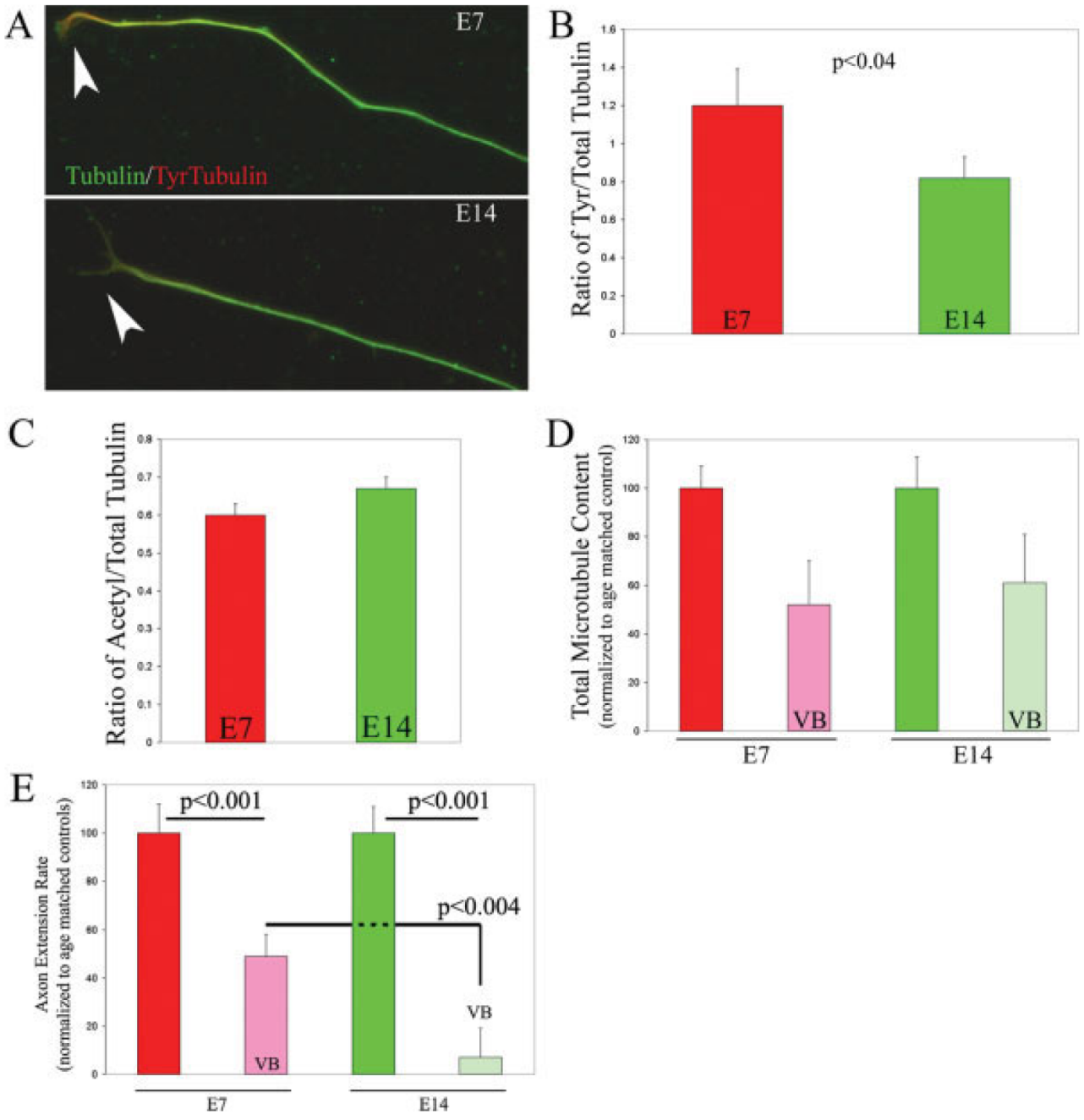

Figure 5.

Analysis of tubulin post-translational modifications in E7 and E14 axons. E7 and E14 DRG explants were cultured on substrata coated with polylysine and laminin and fixed 24 h after plating. Cultures were subsequently doubled labeled for total tubulin and either of two posttranslationally modified forms of tubulin that correlate with changes in net microtubule dynamics (see text). (A) Relative to E7 axons, E14 axons exhibited decreased levels of tyrosinated tubulin. Note the greater relative abundance of tyrosinated tubulin (red) in the distal portion (arrowheads) of the E7 axon relative to the E14 axon. (B) Quantification of the ratio of tyrosinated tubulin to total tubulin in the distal 20 μm of axons (n = 46 and 35 for E7 and E14 axons, respectively). The ratio was decreased in E14 relative to E7 axons ($p < 0.04$). (C)

Quantification of the ratio of acetylated tubulin to total tubulin in E7 ($n = 60$) and E14 ($n = 30$) axons. No difference was observed between the two ages ($p > 0.4$). (D) Decrease in total microtubule content in the distal 40 μm of axons in response to 6 n*M* VB (20 min) as a function of developmental age. Within age, data are normalized to the age matched control revealing the percentage decrease relative to controls. VB treatment depolymerized microtubules to a similar extent at both ages ($p > 0.7$ for comparison of normalized percent decrease across ages). For E7, n = 31 and 30 for control and VB treatment, respectively. For E14, n = 25 and 20 for control and VB treatment, respectively. (E) Treatment with 1 n*M* VB resulted in a greater inhibition of E14 axon extension rate than E7 axon extension rate. $n = 44–48$ axons per group. Extension rates were determined before and after treatment with VB. VB inhibited extension of both E7 and E14 axons ($p < 0.001$ for both comparisons). However, the relative percent of inhibition of axon extension rate, normalized to age matched pre-treatment rates, was significantly greater for E14 axons relative to E14 ($p < 0.004$). [Color figure can be viewed in the online issue, which is available at www.interscience.wiley.com.]

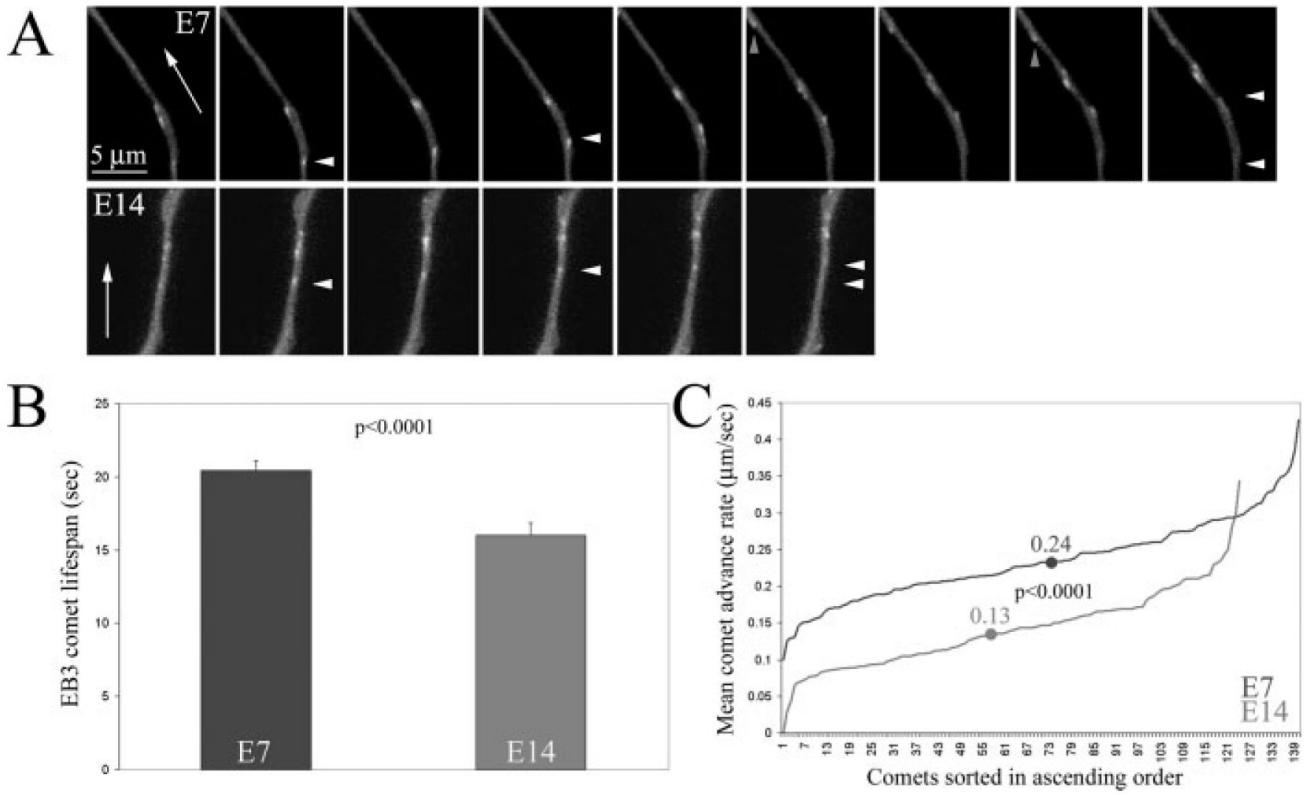

Figure 6.

Determination of microtubule tip polymerization in E7 and E14 axons expressing EB3-EGFP. (A) Examples of EB3 comets in E7 and E14 axons. Three seconds elapse between panels in the sequences. Arrows in the leftmost panels indicate anterograde direction. White arrowheads in panels denote EB3 comets. The gray arrows in the E7 sequence denote one of the rare retrogradely translocating comets (Stepanova et al., 2003), not included in our analysis. The white arrowheads in the last panel of each sequence denote the initial (bottom) and final (top) position of the comet. (B) Quantification of the lifespan of EB3 comets (s) revealed that E14 comets lifespans are 25% shorter than those E7 comets. (C) Measurement of the advance rate of EB3 comets revealed a significant decrease in E14 axons relative to E7. The lines represent the individual comet data sorted in ascending order. The dots on the lines represent the mean for each group. The mean advance rate of E14 comets was 46% slower than that of E7 comets.